



Removal of Cr(VI) by Immobilized Consortium of Freshwater Microalgae in Batch and Continuous System

JASTIN SAMUEL, MADONA LIEN PAUL, JYOTI KUMARI, K.V.G. RAVIKUMAR, CHANDRASEKARAN NATARAJAN and AMITAVA MUKHERJEE*

Centre for Nanobiotechnology, VIT University, Vellore-632 014, India

*Corresponding author: Tel: +91 416 2202620; E-mail: amit.mookerjee@gmail.com

Received: 14 May 2014;

Accepted: 6 August 2014;

Published online: 17 March 2015;

AJC-16985

The potential of an adsorption coupled reduction process for removal of chromium(VI) was evaluated using immobilized algal consortium (of fresh water isolates, *Oocystis*, *Nostoc*, *Syncoccus* and *Desimococcus* species) through batch reactor studies. The batch sorption capacity of algae was substantially enhanced on adaptation to Cr(VI) and consortium formation (83.53 mg/g). The batch data followed Langmuir isotherm and pseudo first order kinetics. The effective applicability of the sorbent for Cr(VI) removal was tested in packed bed column reactor. At the adsorbent dosage of 1 g/L, flow rate of 3 mL/min, bed height of 20 cm and initial Cr(VI) concentration of 300 mg/L, maximum adsorption capacity of 579.2 mg/g was achieved. The possible mechanism of adsorption and reduction of Cr(VI) was explained by Fourier transform infrared spectroscopy and electron paramagnetic resonance spectroscopy analysis confirmed the reduction of Cr(VI) to Cr(III) on the sorbent surface.

Keywords: Algal consortium, Immobilized alginate beads, Surface reduction, Cr(VI) removal.

INTRODUCTION

Chromium(VI) is a hazardous heavy metal found in industrial effluents of electroplating and leather tanning industries¹. Biosorption is considered to be an efficient technique to remove metals from contaminated water because of high efficiency for absorbing metals, environment-friendly, wide operational range of pH and temperature and easy recycling of sorbent². According to earlier reports, in 18th and 19th centuries, living biomass used to be employed for the removal of metals from aqueous solutions^{3,4}. In early 1900's, Arden and Lockett cleaned up the raw sewage in an aeration tank using certain types of living bacterial biomass^{5,6}. The first quantitative study was done on the uptake of copper by fungal spores on metal biosorption of *T. tritici* and *U. crameri* by Hecke in 1902. However, availability and selection of low cost biosorbent material is still a major challenge for environmental biotechnologists.

The algae based wastewater treatment systems (phytoremediation) can provide a sustainable solution for the treatment of municipal and industrial wastewater. They are inexpensive and known for their ability to achieve a good removal of sewage nutrients, pathogens and organic pollutants⁷. However, separation of algal biomass from the treated effluent in these treatment systems by non cost effective industrial filtration and centrifugation pose problems. The immobilization of algal cells into a matrix, can offer a feasible alternative to filtration

and centrifugation⁸. The immobilization also increases the retention time of cells in aqueous medium which helps the cells to adapt to substrate and keeps the metabolic activity constant for a long period⁹. Immobilization of *Spirulina platensis* and *Bacillus sp.* in alginate matrix for biosorption has been investigated^{1,10}. The immobilization technique helps the biosorbent to have a better shelf life and offers easy and convenient usage compared to free biomass which is easily biodegradable¹¹. To minimize the cost, low concentrations of high molecular-weight grades of non toxic sodium and calcium salts of alginates are employed as biosorbents^{12,13}.

The process engineering advantages of a packed bed adsorption column with immobilized biomass offer ease of scalability. The modeling of column reactor data facilitates scale-up potential. There are few reports on the modeling of packed bed column using immobilized algae for heavy metal removal. The *S. platensis* was immobilized in alginate beads for biosorption of chromium¹. The removal of mercury from aqueous solution by a packed-bed reactor (PBR) containing *Chorella emersonii* entrapped in alginate and agarose gels was studied by Robinson and Wilkinson¹⁴. A laboratory scale algal column reactor with green microalgae, *Chlorella vulgaris*, immobilized in alginate beads was used by Lau and co-workers to treat copper and nickel¹⁵.

Different algal species such as *Ulva lactuca*, *S. platensis*, *Spirogyra sp.*, *Cladophora albida*, *Chroococcus*, *Nostoc*

caldicola, *Chlorella* and *Sargasam sp* have been previously explored for removal of Cr(VI) (Table-1).

In the previous studies, substantial removal of Cr(VI) was demonstrated by consortium formation of indigenous chromite mine bacterial isolates^{16,17}. Since the microalgae are widely exploited sorbents for different contaminants, the current study was aimed to explore the potential of a consortium of freshwater algae, from a pristine non contaminated source, as an effective bio-sorbent for Cr(VI). The calcium alginate gel was used for immobilization of the algal consortium (*Oocystis*, *Nostoc*, *Syncoccus* and *Desimococcus* species) by the entrapment technique. The optimization of the batch sorption parameters, equilibrium studies were carried out. The mechanism of sorption was studied through BET, FT-IR, SEM-EDX and EPR. The possible surface reduction of adsorbed Cr(VI) to less toxic Cr(III) was also studied to investigate the detoxification potential of the process. The reusability of the sorbent system was determined by four cycles of intermittent adsorption/desorption cycle. The application potential of the algal consortium immobilized sorbent was tested in continuous flow reactor using Cr(VI) spiked aqueous matrices.

EXPERIMENTAL

Preparation and immobilization of algal consortium: The algae, *Oocystis sp*, *Nostoc sp*, *Syncoccus sp* and *Desimococcus sp* were isolated from Retteri Lake, Chennai, India and grown in BG 11 broth under shaking condition (120 rpm) at 30 °C. The concentration of chromium in lake water measured by Atomic absorption spectrophotometer (AAS) was below detection level. The genus level identification was done with the help of Centre for Advanced Studies (CAS) in Botany, University of Madras, India. The algal cells were adapted sequentially from 1-100 mg/L of Cr(VI). The adapted algal isolates were tested for antagonistic/synergistic effect. The adapted algal cells having synergistic effect were grown together as consortium. In deviation from the previous methods of bio-sorption studies of biosorption by single algal culture (Table-1) an algal consortium was developed to enhance the Cr(VI) sorption capacity. For sorption study, the algal cells were grown

both as individual and consortium. The cells were harvested by centrifuging the algal culture media at 4,000 × g for 20 min. The collected algal cells were washed using double distilled water before conducting the sorption experiments.

A 4 % (w/v) slurry of sodium alginate was prepared by continuous stirring in hot (60 °C) distilled water. A 4 % (w/v) of adapted algal consortium was added to sodium alginate slurry after cooling and stirred. The alginate-adapted algal consortium was then extruded using a 0.45 mm × 13 mm gauge syringe into 0.2 M CaCl₂·2H₂O as a cross linking agent for polymerization and immobilized bead formation. The beads were of 1 mm diameter and were kept in the polymerizing medium for 4 h at 4 °C. Then the beads were washed in saline and distilled water to remove the unbound or loosely bound CaCl₂¹⁷. In another novel development, the algal consortium was immobilized to improve the Cr(VI) sorption capacity obtained by free cells of algal consortium.

Suspended/immobilized batch reactor studies: The adsorption of chromium by individual algal sp (*Oocystis sp*, *Nostoc sp*, *Syncoccus sp* and *Desimococcus sp*), adapted algal consortium and adapted algal consortium immobilized alginate beads were carried out in batch. The batch studies were conducted for biosorption at initial Cr(VI) concentration of 100 mg/L and 100 mg sorbent dose in 100 mL metal solution at 30 °C for 180 min at pH varying from 2.0-7.0 by adding 0.01 N HCl. The effect of contact time was studied at initial Cr(VI) concentration of 100 mg/L and 100 mg sorbent dose in 100 mL solution at 30 °C and optimized pH. The samples were analyzed for Cr(VI) at time intervals of 30, 60, 90, 120, 180 and 240 min. The effect of temperature on sorption was determined through batch experiments carried out at different temperatures (25, 30, 35, 40 and 45 °C). The effect of temperature on Cr(VI) solubility was tested by control experiments conducted in the absence of sorbent. The batches of sorption studies were carried out at optimized sorption parameters and 100 mg sorbent dose in 100 mL metal solution for different initial Cr(VI) concentrations in the range of 5-300 mg/L to determine the variation in sorption with initial metal ion concentration. The sorbent dosage was optimized by varying the sorbent dosage at 25, 50, 100, 200, 300 and 400 mg in 100 mL metal solution of 100

TABLE-1
COMPARATIVE Cr(VI) ADSORPTION USING BIOMASS IMMOBILIZED ALGINATE BEADS. THE CURRENT STUDY SHOWS HIGH ADSORPTION CAPACITY

Initial conc. (mg/L)	Heavy metal	Adsorbent	Adsorbent dose	pH	Temp. (°C)	Time (min)	Adsorption capacity	Reference
5-50	Cr(VI)	<i>Ulva Lactuca</i> (dry)	–	1	25 ± 2	120	10.61	49, 50
5-250		<i>Ulva</i> activated carbon	–	1	26 ± 2	121	112.6	
25-250	Cr(VI)	Spent Biomass <i>S.platensis</i> fresh biomass <i>S.platensis</i>	0.2-2.4 g/L	1.5	25	5-600	213 189	54
5	Cr(VI)	Filamentous algae <i>Spirogyra sp</i>	5,10,15 g/L	2	18	120	14.7 mg/g	25
154	Cr(VI)	Non-living green algae <i>Cladophora albidia</i>	2 g/L	2	45	500	41.7 mg/g	53
20	Cr(VI)	<i>Chroococcus</i> <i>Nostoc calcicola</i>	– 1 g/L	4 3	26	30	210.37 mg/g 21.36 mg/g	19
100	Cr(VI)	<i>Chlorella</i> + NaAlg	60 % w/v	2	30	30 h	57.33 mg/g	2
250	Cr(VI)	<i>Sargasam Sp</i> dried biomass	–	2	–	12 h-equ	19.06 mg/g	51, 52
100	Cr(VI)	<i>Spirulina platensis</i> 1 mm alginate beads	–	1.5	–	180	372.27 mg/g	1
300	Cr(VI)	<i>Oocystis</i> , <i>Nostoc</i> , <i>Syncoccus</i> , <i>Desimococcus</i> consortia immobilized in alginate beads	0.9 g/L	3	30	190	579.2 mg/g	Current study

mg/L of Cr(VI). Each experiment was carried out in triplicates and the results are given as the mean value \pm SD.

The metal sorption efficiency of biosorbent was determined by the sorption capacity which is given as the amount of metal ions adsorbed per unit biosorbent (mg metal ions g⁻¹ dry biosorbent). The sorption capacity and the percentage of biosorption by the biosorbent were obtained by the following equations:

$$q = \frac{V(C_0 - C_e)}{m} \quad (1)$$

$$\text{Biosorption (\%)} = \frac{(C_0 - C_e)}{C_0} \times 100 \quad (2)$$

where, q is the sorption capacity in mg/g, V is the volume of solution (L), C_0 is the initial Cr(VI) concentration in mg/L, C_e is the Cr(VI) concentration at equilibrium and m is the weight of biosorbent (g).

The adsorption isotherms explain the interaction of a sorbate molecule to the sorbent and are considered as a critical parameter for designing sorption systems. The adsorption equilibrium data at 30 °C were modeled using Langmuir, Freundlich and Dubinin-Radushkevich isotherms to study the mode of interaction of Cr(VI) ions with sorbent when the metal solution phase and sorbent solid phase are in equilibrium.

The dynamics of sorption process describes the rate at which a solute gets adsorbed onto the biosorbent. Different models have been used to describe the metal uptake rate. The pseudo-first order and pseudo-second order models were applied to the sorption data. The model with the highest correlation coefficient value (R^2) close to unity was considered the best fit.

The thermodynamic parameters such as changes in standard free energy (ΔG°), standard enthalpy (ΔH°) and standard entropy (ΔS°) were calculated for the evaluation of feasibility of the adsorption reaction and to fully understand the nature of adsorption. It was possible to estimate these thermodynamic parameters for the adsorption reaction by considering the equilibrium constants under several experimental conditions.

Characterization of algal consortium immobilized alginate beads: Surface area, pore volume, pore diameter and porosity of the alginate beads and adapted algal consortium immobilized alginate beads were determined with a BET analyzer (Micromeritics Autopore IV, USA). The isotherm plots were used to calculate the specific surface area (N2/BET method) and average pore diameter of the beads, while pore volume was calculated from the volume of nitrogen adsorbed at p/p_0 0.999.

The surface morphology of algal consortium immobilized alginate beads were studied under scanning electron microscope. The interacted and uninteracted algal consortium immobilized alginate beads were dried and mounted on 10 mm metal stubs using a carbon tape. The samples were then sputtered coated with gold under vacuum in argon atmosphere. The analysis was made using potential difference of 20 kV for the tungsten filament. The surface morphology of the coated sample was observed by a scanning electron microscope (Hitachi S400, Japan).

The surface elemental analysis of Cr(VI) interacted and uninteracted algal consortium immobilized alginate beads was

carried out by energy dispersive X-ray spectroscopy. The gold sputtered samples were analyzed and the spectra were recorded using JEOL JSM-5510 equipments.

The surface chemical characteristics of the biosorbent were characterized by IR Affinity-1 Fourier transform-infrared spectrometer (Shimadzu, Japan). The Cr(VI) interacted and uninteracted algal consortium immobilized alginate beads were each mixed with 100 mg KBr and the fine powdered consortium was then pressed in a mechanical die press to form a pellet by applying a pressure of 1200 psi for 5 min. The transparent tablets were inserted in the instrument and the spectra were recorded from 4000-400 cm⁻¹.

The solid state spectra of algal consortium immobilized alginate beads interacted and uninteracted with Cr(VI), was recorded at room temperature by Varian E-112 Electron Paramagnetic Resonance spectrometer (9.5 GHz) operating at X-band frequency with a 100 kHz modulation frequency. The spectrum was recorded under the following conditions: microwave power: 3.1 mW, modulation amplitude: 3 G.

Application studies in immobilized bed continuous flow reactor: The continuous sorption experiments were conducted in a glass column (1.5 cm ID and 30 cm height), packed with a known quantity of adapted algal consortium immobilized alginate beads. A 100 mg/L of Cr(VI) solution was pumped through the column, at desired flow rates using a peristaltic pump. The optimized parameters were used for the algal consortium immobilized alginate beads. The Cr(VI) concentration was quantified at each interval from the sampling point. The packed bed column study was carried out at pH 3.0 and 30 °C temperature.

The total quantity of Cr(VI) adsorbed in the column (W_{ad}) is calculated from the area above the breakthrough curve [outlet Cr(VI) concentration vs. time] multiplied by the flow rate. The adsorption capacity (q) of algal consortium immobilized alginate beads is calculated on dividing W_{ad} by sorbent mass (M). The total amount of Cr(VI) ions entering the column can be calculated from the eqn. 1:

$$W = \frac{C_0 \cdot F \cdot t_e}{1000} \quad (3)$$

where, C_0 is the inlet Cr(VI) concentration (mg/L), F is the volumetric flow rate (mL/h) and t_e is the exhaustion time (h). The total Cr(VI) removal percentage can be calculated from the equation:

$$\text{Total Cr(VI) removal percentage} = \frac{W_{ad}}{W} \times 100 \quad (4)$$

The effect of flow rate on Cr(VI) adsorption was studied by varying the flow rates, 3, 9 and 15 mL/min, keeping bed height and initial Cr(VI) concentration constant at 10 cm and 100 mg/L, respectively. The effect of bed height on sorption of Cr(VI) was evaluated by varying the bed height, 10, 15 and 20 cm, while, flow rate and inlet Cr(VI) concentration were constant at 3 mL/min and 100 mg/L, respectively. The effect of influent Cr(VI) concentration on breakthrough point and sorption capacity was studied by varying influent Cr(VI) concentration, 100, 200 and 300 mg/g, respectively keeping the bed height and flow rate (20 cm and 3 mL/min) constant.

The reusability of biosorbent was studied by four cycles of alternating sorption/desorption experiments with the

supplement of 300 mg/L of Cr(VI) at the beginning of each cycle. About 0.01 N NaOH was used to desorb Cr(VI) from column.

Treatment of Cr(VI) spiked natural water and tannery effluents: The application of optimized Cr(VI) sorption was investigated in different natural water and tannery effluent matrices. The samples from different locations [ground water (GW1, GW2) and effluent water (T1, T2)] from Soloor and Suthipattu in Vellore, India; lake water (freshwater) and domestic waste water from VIT University, Vellore, India) were collected and adsorption experiments were carried out at optimized pH 3, 30 °C temperature, 1 g/L sorbent (algal consortium immobilized alginate beads) dosage and equilibrium time 180 min. The initial Cr(VI) concentration of 300 mg/L was spiked in all the samples. Both initial and final concentrations of Cr(VI) were studied by 1,5-diphenyl carbazide assay. The total Cr was quantified by atomic absorption spectrophotometer. The Cr (III) concentration was calculated by the difference in total Cr and Cr(VI).

Statistical analysis: Each set of experiment was carried out in triplicates. One-way Anova with Dunnett's post test and Tukey's Multiple Comparison Test was carried out using GraphPad Prism 5.0 software to check statistical significance of the results obtained experimentally.

RESULTS AND DISCUSSION

BET analysis: The algal consortium immobilized alginate beads had a higher surface area of 1.980 m²/g compared to alginate beads (0.1298 m²/g). The average pores size of the beads containing algal consortium was 709.34 Å and the total pore volume at $p/p_0 = 0.999$ was 0.0035 cm³/g. These results agree with those from the similar studies carried out on Cr(VI) adsorption by immobilized bacterial consortium-alginate bead and immobilized *Rhizopus*-alginate beads^{17,39}.

Conditions effecting sorption in batch reactor: The pH of solution determines both speciation of Cr(VI) in aqueous medium and binding site availability on the sorbent surface. The Cr(VI) adsorption capacity of algal consortium immobilized alginate beads increased from 42.81 mg/g at pH 2.0-71.25 mg/g at pH 3.0 and decreased gradually to 5.69 mg/g till pH 7.0 (Fig. 1A). At a lower pH range of 1.0-4.0, Cr(VI) predominantly exists in the form of monovalent HCrO₄⁻ and is likely to get adsorbed on the positively charged biosorbent surface. The optimum pH 3.0 obtained for algal consortium immobilized alginate beads is well in agreement with the previous studies carried out in different type of alginate beads^{18,19}.

The sorption capacity of Cr(VI) by algal consortium immobilized alginate beads increased steadily up to 71.25 mg/g as the contact time increased from 30-180 min (Fig. 1B). This study shows that a maximum amount of Cr(VI) was adsorbed within the first 180 min. The sorption capacity stabilized beyond 180 min. The maximum adsorption within 180 min may be due to the excess availability empty sites initially. The constant sorption capacity after 180 min indicates equilibrium conditions due to lack of active sites left for further sorption.

The sorption capacity increased initially with an increase in temperature from 25-30 °C (Fig. 1C) and decreased as the

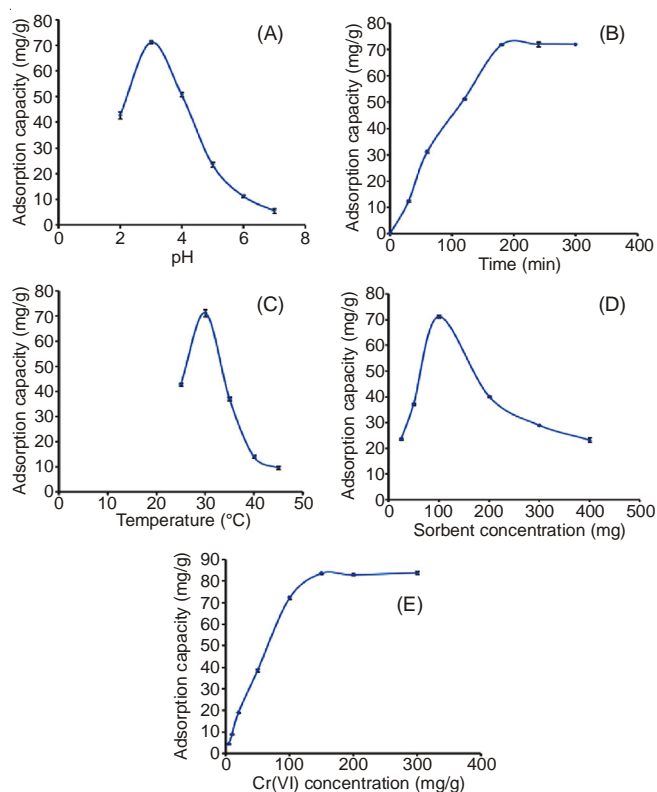


Fig. 1. (A) Effect of pH (B) contact time (C) temperature (D) biosorbent concentration (E) initial Cr(VI) concentration on the sorption capacity of Cr(VI) by algal

temperature was increased up to 45 °C. The non-significant difference in Cr(VI) concentration in the control samples at time 0 and 3 h was noted indicating the negligible impact of temperature on Cr(VI) solubility. The maximum sorption capacity of 71.25 mg/g was obtained at 30 °C. This is similar to the earlier reports on optimum temperature for Cr(VI) adsorption by alginate beads^{2,20}. The initial increase in the adsorption capacity of sorbents with increasing temperature may be due to the generation of more number of active sites on the sorbents with temperature. The decrease in sorption capacity beyond 45 °C may be due to the loss in binding sites.

A maximum chromium (VI) sorption capacity of 71.25 mg/g was observed when 1 g/L of algal consortium immobilized alginate beads were used (Fig. 1D). With increase in the sorbent dosage of algal consortium immobilized alginate beads from 0.25 to 1.0 g/L, an increased sorption capacity from 5.88 to 71.25 mg/g was observed. The sorption capacity decreased from 71.25 to 23.14 mg/L as the sorbent dosage increased from 1 to 4 g/L. The increase in sorption capacity with increase in sorbent dosage is due to the availability of sorption sites. The decrease in sorption capacity with increase in sorbent dosage more than 1 g/L may be due to the decrease in available metal ion compared to the increase in sorption sites²¹.

The sorption capacity of algal consortium immobilized alginate beads increased from 4.45 to 83.53 mg/g with an increase in Cr(VI) concentration from 5 to 150 mg/L for a constant sorbent dosage used (1 g/L) after which it remained constant (Fig. 1E). As the initial Cr(VI) concentration was increased to 300 mg/L, there was no significant increase in sorption capacity ($p < 0.5$). The initial increase in sorption

capacity may be due to more availability of the metal ions. Moreover, a high initial Cr(VI) concentration exerts a driving force to overcome the mass transfer resistance between solid and aqueous phase²². The lack of substantial increase in the sorption capacity with an increase in Cr(VI) concentration may be due to the saturation of available binding sites on the sorbent^{2,23}.

The sorption capacity of adapted algal consortium immobilized alginate beads employing the optimized conditions (pH: 3.0, contact time: 180 min, temperature: 30 °C, initial Cr(VI) concentration: 150 mg/L, sorbent dosage: 1 g/L) was 83.53 mg/g. A statistically significant increase in the sorption capacity of adapted algal consortium immobilized alginate beads compared to unadapted individual algal sp [*Oocystis* (16.97 mg/g), *Nostoc* (19.37 mg/g), *Syncoccus* (20.3 mg/g) and *Desimococcus* sp (24.5 mg/g)], unadapted algal consortium (38.35 mg/g) and adapted un-immobilized algal consortium (49.23 mg/g) could be confirmed by One-way ANOVA and Dunnett post test (p value: 0.0001). The biosorption capacity of algal consortium immobilized in alginate beads (83.53 mg/g) in the current study is remarkably high in a short time (3 h) compared to the batch sorption capacity of 57.33 mg/g reported for single algal sp *Chlorella* immobilized² in alginate beads at pH 2, temperature 30 °C and time 30 h. Also the sorption capacity reported in the current study (83.53 mg/g) is more than the sorption capacity of 14.7 and 21.36 mg/g reported for the free cells of *Spirogyra* sp and *Nostoc calcicolla*^{19,47}. This validates that the consortium formation and immobilization enhanced the Cr(VI) sorption capacity of fresh water algae.

Sorption isotherms, thermodynamics and kinetics: The adsorption equilibrium data at 30 °C were modeled using Langmuir, Freundlich and Dubinin-Radushkevich isotherms (Table-2). The best fit was obtained in the case of Langmuir model (r^2 0.997) with q_0 value 90.9 mg/g. The theoretically quantified sorption capacity from the Langmuir plot was close to the results obtained by sorption experiments. The Langmuir model of adsorption observed in the current study is based on the surface homogeneity. This suggests that even at the unavailability of sufficient sorption sites as in the case of algal consortium immobilized alginate bead, a monolayer of sorption devoid of interaction between sorbed molecules is highly probable. The adsorption of Cr(VI) by indigenous cyanobacteria immobilized alginate beads, bio-polymeric beads of cross linked alginate and gelatin, ethylenediamine-modified cross-linked magnetic chitosan resin, were reported to follow Langmuir isotherm^{19,20,24}.

The temperature dependent parameters, change in free energy, enthalpy and entropy were quantified (Table-3). The negative ΔG , ΔH and positive ΔS value for the sorbent suggests that the sorption process is spontaneous. In addition, the positive value of ΔS implies a favorable adsorption²⁰.

Parameter	Algal consortium immobilized alginate beads
Langmuir constants	
q_0 (mg/g)	90.9
b (L/mg)	0.126
r^2	0.997
Freundlich constants	
K_f (mg/g)	14.15
n (L/mg)	2.59
r^2	0.875
D-R constants	
q_D (mg/g)	1.22
B_D (mol ² /KJ ²)	0.029
E_D (KJ/mol)	4.1
r^2	0.91

Temperature (°C)	Algal consortium immobilized alginate beads	
	ΔG (KJ/mol)	
25	-1.976	
30	-1.989	
35	-2.009	
40	-2.042	
45	-2.075	
ΔH (KJ/mol)	-3.764	
ΔS (KJ/mol/K)	0.018	

The rate constant values obtained for pseudo first order and pseudo second order, k_1 and k_2 are tabulated (Table-4). The correlation coefficient r^2 value suggests that the system fits better to pseudo first order than the pseudo second order. The sorption kinetics following pseudo first order rate equation indicates that, in the presence of a large excess of Cr(VI) ions, the rate of sorption is highly dependent on the biosorbent capacity which is a function of the number of available sites for binding or ion exchange. Therefore, the rate limiting steps for sorption was the biosorbent capacity^{25,26}.

Mechanistic studies

SEM-EDX: The SEM images of Cr(VI) interacted and uninteracted algal consortium immobilized alginate beads were taken at 200 \times , 130 \times magnification, respectively (Fig. 2A, C). The SEM images were magnified to observe the surface of adsorbent. At 3000 \times magnification, surface roughness and ridges were visible for algal consortium immobilized alginate beads (Fig. 2B). The decrease in the surface roughness after interaction of algal consortium immobilized alginate beads with Cr(VI) correlates with the unavailability of sorption sites after equilibrium of sorption (Fig. 2D). The EDX spectra provides

Biosorbent	Pseudo first order			Pseudo second order		
	k_1 (min ⁻¹)	q_e (mg/g)	r^2	k_2 (g/mg/min)	q_e (mg/g)	r^2
Algal mixture immobilized beads	0.002	82.22	0.994	0.00002	125	0.877

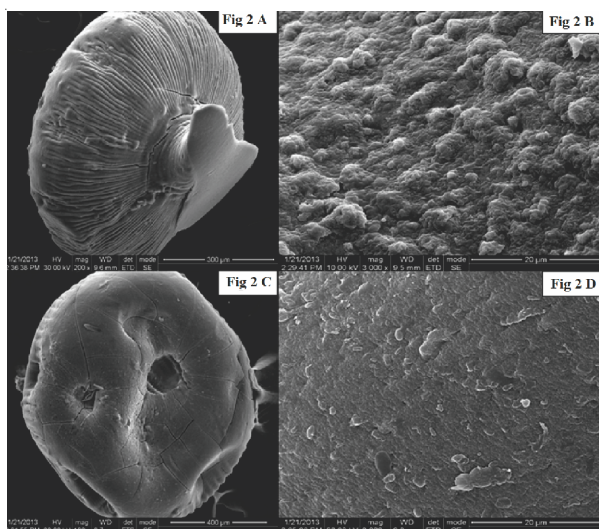


Fig. 2. SEM images of (A) algal consortium immobilized alginate beads at 110x magnification (B) 3000x magnified view of algal consortium immobilized alginate beads (C) Cr(VI) interacted algal consortium immobilized alginate beads at 130 x magnification and (D) 3000x magnified image of Cr(VI) interacted algal consortium immobilized alginate beads

information on the elemental composition of the surface analyzed (Fig. 3A,B). The spectrum obtained for interacted algal consortium immobilized alginate beads confirms the presence of chromium ions on the sorbent surface.

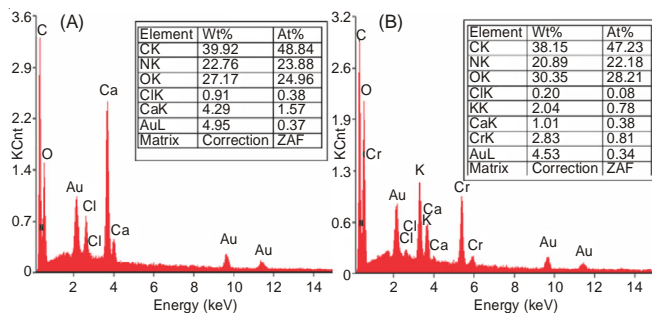


Fig. 3. EDX spectra of (A) uninteracted (B) Cr(VI)-interacted alginate beads containing algal consortium

FT-IR Studies: The biosorptive interaction of Cr(VI) with the algal consortium immobilized in alginate beads were investigated by the FTIR technique. The major IR absorption bands of the algal consortium immobilized in alginate beads are saccharides and peptides. The binding of metal ions to microbe relates to oxygenous or nitrogenous functional groups on the cell wall biopolymers of algal biomasses^{27,28}. The IR spectra of un-interacted and Cr(VI) adsorbed algal consortium immobilized in alginate beads are shown, respectively in Fig. 4(A) and (B). The spectrum of the uninteracted biosorbent displays absorption bands near 1654 and 1438 cm⁻¹, respectively due to the asymmetrical and symmetrical C(=O) stretching bands of the carboxylate ion group (COO⁻) of terminal amino acid^{29,30}. After the interaction with Cr(VI), the algal consortium immobilized in alginate beads exhibited the spectrum with clear changes of the asymmetrical C(=O) stretching band at 1654 cm⁻¹ disappearing and its symmetrical stretching band at 1438 cm⁻¹ weakening. These changes are

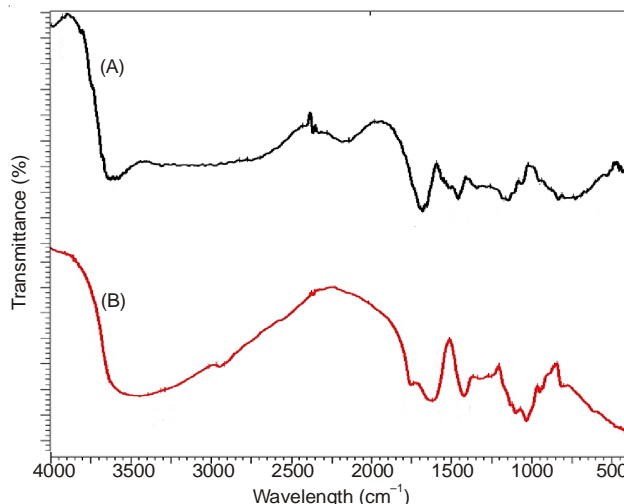
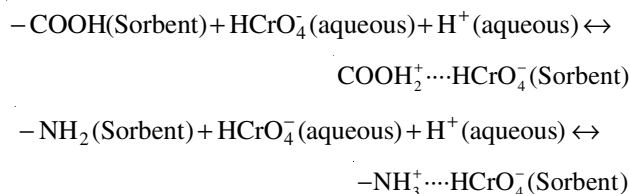


Fig. 4. FTIR spectra of (A) uninteracted (B) Cr(VI)-interacted alginate beads containing algal consortium

typical of the complexation of the carboxylate anion functional group by coordination with metal cations³¹. In this case, most of the carboxylate ion had complexed or chelated with Cr because the asymmetrical stretching band at 1654 cm⁻¹ moved to a lower frequency³¹, which may be overlaid by other lower frequency bands, resulting in deepening the peak valley between 1614 and 1417 cm⁻¹ and the symmetrical C(=O) stretching band at 1438 cm⁻¹ moved to a lower frequency³¹, which may also be concealed by other lower frequency bands, resulting in the intensity of the band to be weakened. Another shift can be observed from 1170 and 1099-1047 and 1029 cm⁻¹, respectively with increase in peak intensity, corresponding to the interaction of Cr with the oxygen of the hydroxyl group (C-O-H)³¹ from saccharides. The increase in intensity at 3653 to 3390 cm⁻¹ with peak shift after interaction with Cr(VI) is due to the phenol and amine groups (NH) in algal biomass. A broad and moderately intense peak was visible at the range of 810.1 cm⁻¹ representing Cr-O vibrations which were absent in the uninteracted beads³².

The possible mechanism of Cr(VI) adsorption,



A new absorption band at 1747 cm⁻¹ corresponding to the C=O stretching band $\nu(\text{C}=\text{O})$ of the carboxyl group occurred in Cr(VI) interacted algal consortium immobilized in alginate beads. There are two possibilities that account for the occurrence of the new band of the carboxyl group. However a considerable enhancement of the intensity with peak shift of both the absorption bands at 3653-3390 and 1099-1029 cm⁻¹, respectively due to the $\nu(\text{O}-\text{H})$ and $\delta(\text{O}-\text{H}) + \nu(\text{C}-\text{O})$ of the hydroxyl group from saccharides, is observed in Fig. 4, which shows that the free hydroxyl group increased. The result made clear that some polysaccharides on the peptidoglycan layer of the algal cell wall had hydrolyzed to shorter saccharides such as oligosaccharides, dises and monoses. It is well understood

that the mechanism of the Cr biosorption involves an apparent redox reaction, the Cr(VI) is reduced to the Cr(III) form (Fig. 5). The occurrence of the new carboxyl absorption band in IR is likely due to the oxidation of the free aldehyde group of the hemiacetalic hydroxyl group from the reducing sugars. Since the proton of the system can't directly affect the IR absorption of the carboxyl in this case, one of the primary causes of the two distinctly enhanced intensities of the carboxyl absorptions at 1747 cm^{-1} $\nu(\text{C}=\text{O})$ and 947 cm^{-1} $\delta(\text{O}-\text{H})$ in Fig. 4 is thought to involve the oxidation of the reducing sugars to their corresponding acids by the heavy metal cation³².

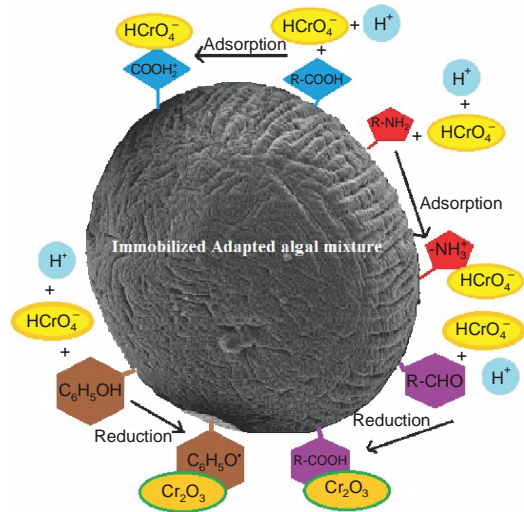


Fig. 5. Adsorption coupled reduction mechanism of Cr(VI) removal by immobilized algal consortium

The possible mechanism of Cr(VI) reduction,

- (i) $\text{R-CHO} + 2\text{HCrO}_4^- (\text{sorbent}) + 2\text{H}^+ (\text{aqueous}) \rightarrow \text{R-COOH} (\text{sorbent}) + \text{Cr}_2\text{O}_3 (\text{sorbent}) + 2\text{H}_2\text{O} (\text{aqueous})$
- (ii) $\text{C}_6\text{H}_5\text{OH} + 2\text{HCrO}_4^- (\text{sorbent}) + \text{H}^+ (\text{aqueous}) \rightarrow \text{C}_6\text{H}_5\text{O}^- (\text{sorbent}) + \text{Cr}_2\text{O}_3 (\text{sorbent}) + 2\text{H}_2\text{O} (\text{aqueous})$

EPR Analysis: In order to confirm the redox reaction of the reducing agents on Cr(VI), EPR analysis was conducted for Cr(VI) interacted (Fig. 6A) and non-interacted (Fig. 6B) algal consortium immobilized alginate beads to understand the possible valence states of chromium after sorption. The peak centered at a g factor of 2.14 was observed in Cr(VI) interacted algal consortium immobilized alginate beads, which could be attributed to Cr(V) paramagnetic signal. A peak at g factor of 1.98 observed in Cr(VI) interacted algal consortium immobilized alginate beads could be attributed to Cr(III) paramagnetic signal³³. This demonstrates the possible reduction of Cr(VI) to Cr(III) on the surface of sorbent after adsorption.

Speciation of Cr released from Cr loaded sorbent: After equilibrium sorption, the Cr(VI) loaded algal consortium immobilized alginate beads were collected and suspended in distilled under optimized sorption parameters without Cr(VI). The setup was kept in shaker for 240 h and the samples were collected at 24 h interval and analyzed for Cr(VI) and Cr(III). The surface adsorbed Cr was found to be released into water. The released Cr was quantified by DPC and AAS. At 24 h 2.63 mg/L of Cr was present in the solution. As the time increased to 192 h the concentration of Cr released from the sorbent increased to 34.52 mg/L (Fig. 7). With further increase in time

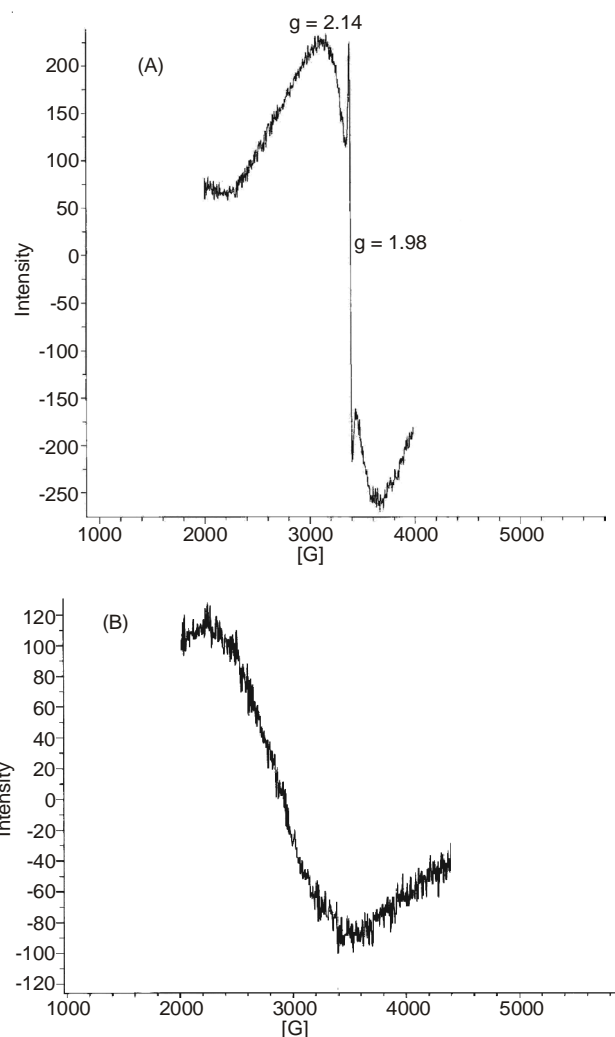


Fig. 6. EPR spectra of (A) Cr(VI)-interacted alginate beads containing algal consortium (B) un-interacted alginate beads containing algal consortia(control)

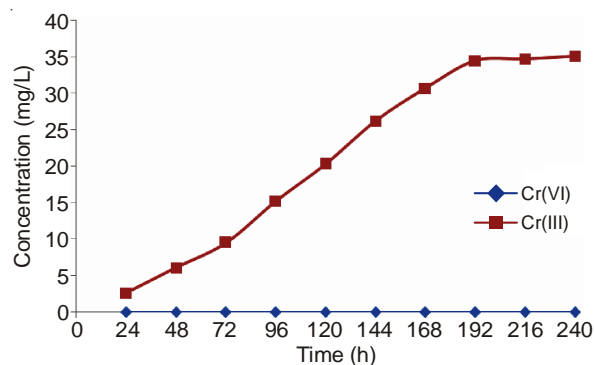


Fig. 7. Speciation of Cr released from the Cr loaded algal consortium immobilized in alginate beads

there was no significant release of Cr from the sorbent. It was found that the released Cr was Cr(III). This corroborates with the EPR results that the adsorbed Cr on the surface of the adsorbent was Cr(III).

Sorption in continuous flow reactor: The breakthrough curve for the sorption of Cr(VI) at different flow rates is shown in Fig. 8A. It was observed that the breakthrough time decreased from 55 min at 3 mL/min to 15 min at 15 mL/min flow rate.

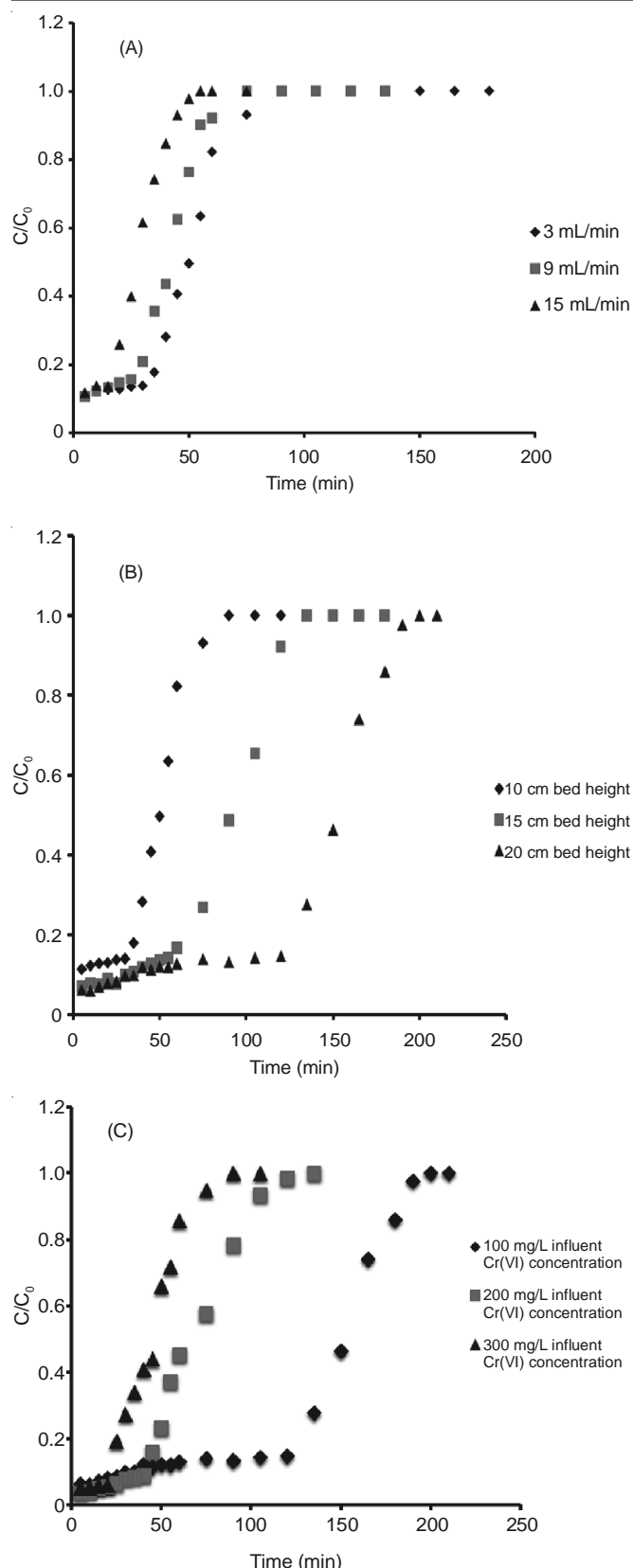


Fig. 8. Effect of (A) flow rate and (B) bed height (C) inlet Cr(VI) concentration in packed bed reactor using alginate beads containing algal consortium

The breakthrough curves for Cr(VI) sorption at different bed heights are given in Fig. 8B. The results show that the breakthrough time and sorption capacity increased from 25 to

120 min and 103.1 to 188.1 mg/g as the bed height increased from 10-20 cm, respectively. The volume of solution processed by 10, 15, 20 cm bed heights are 270, 405 and 600 mL, respectively. The total chromium ions adsorbed by the column increased from 87.66-207 mg as the bed height increased from 10-20 cm.

The effect of influent Cr(VI) concentration on the breakthrough curves is shown in Fig. 8C. The breakthrough time decreased with increasing influent Cr(VI) concentration. With increase in influent Cr(VI) concentration from 100 to 300 mg/L, the Cr(VI) adsorbed were found to increase from 188.1 to 579.2 mg/g and the exhaustion time for the sorbent decreased from 200 to 90 min. A decrease in Cr(VI) concentration gave a delayed breakthrough curve. The maximum adsorption capacity of algal consortia immobilized alginate bead was 579.2 mg/g at 300 mg/L influent Cr(VI) concentration, 20 cm bed height and 3 mL/min flow rate.

The increase in sorption capacity with influent Cr(VI) concentration can be explained by the fact that the higher concentration gradient facilitated a faster transport owing to an increased diffusion coefficient or mass transfer coefficient^{34,35}. This may be attributed to high influent Cr(VI) concentration providing a higher driving force for the transfer process to overcome the mass transfer resistance³⁶. The increased driving force for mass transfer also ensured that the sorbent achieved saturation earlier resulting in a decrease in the exhaustion time^{36,37}. Similar phenomena of increase in breakthrough time and exhaustion time with decrease in flow rate and increase in bed height have already been reported^{18,38}.

The sorption capacity achieved in the current study is considerably high compared to earlier studies with different types of alginate beads in continuous flow reactor^{10,39,48}. The adsorption capacity achieved in the current study was higher than the maximum reported (372.27 mg/g) for metal removal employing single algae *Spirulina platensis* immobilized in alginate bead¹.

Breakthrough curve modeling in continuous flow reactor:

The Adams-Bohart model provides a simple and comprehensive approach to conduct and evaluate sorption-column test. However, its validity is limited to the range of conditions used^{40,41}. In Adams-Bohart model, the values of k_{AB} increased from 1.9×10^3 - 2.18×10^3 L/mg min as the bed height was increased from 10-20 cm (Table-5). The 50 % breakthrough time (t_{50}) increased from 3.5-5.5 min as the bed height increased. The critical breakthrough point (Z_0) was constant at all bed heights. It shows that the overall system kinetics was dominated by external mass transfer in the initial part of adsorption in the column⁴¹.

The Thomas model (r^2 ranged from 0.910 to 0.961) provided a better fitting compared to the Adams-Bohart model. From Table-6, it is observed that, as the flow rate increased from 3-15 mL/min, the value of k_{TH} increased from 1.25×10^2 to 6.12×10^2 mL/min mg and the value of q_0 decreased from 172.62 to 83.87 mg/g. The Thomas model was suitable for adsorption process, which indicates that the external and internal diffusions were not the limiting step^{36,40,42}.

The different statistical parameters of the Yoon-Nelson model were calculated and given in Table-7. The r^2 values from

TABLE-5
PARAMETERS OF ADAMS-BOHART MODEL UNDER DIFFERENT BED HEIGHT USING LINEAR REGRESSION ANALYSIS OBTAINED WITH $r^2 = 1$

C_0 (mg/L)	Q (mL/min)	Z (cm)	Adams-Bohart		v (cm/h)	t_{50} (min)	Z_0 (cm)	r^2
			$K \times 10^3$ (L/mg min)	N_0 (mg/cm ³)				
100	3	10	1.90368	197.23	909.2	3.5	1.5	0.85
100	3	15	2.14135	200	1000	4	1.5	0.83
100	3	20	2.18004	200	1000	5.5	1.5	0.86

TABLE-6
PARAMETERS OF THOMAS MODEL UNDER DIFFERENT FLOW RATE USING LINEAR REGRESSION ANALYSIS

C_0 (mg/L)	Q (mL/min)	Z (cm)	Thomas		r^2
			$K_{TH} \times 10^2$ (mL/min mg)	q_0 (mg/g)	
100	3	10	1.254	172.62	0.91
100	9	10	3.168	113.48	0.95
100	15	10	6.12	83.87	0.961

TABLE-7
PARAMETERS OF YOON-NELSON MODEL UNDER DIFFERENT INLET Cr(VI) CONCENTRATION AND BED DEPTH USING LINEAR REGRESSION ANALYSIS

C_0 (mg/L)	Q (mL/min)	Z (cm)	Yoon-Nelson		r^2
			K_{YN} (min ⁻¹)	τ (min)	
100	3	20	1.16	120.3	0.91
200	3	20	2.59	58.9	0.95
300	3	20	3.861	25.64	0.96
100	3	10	1.94	50.43	0.91
100	3	15	1.32	72.4	0.88
100	3	20	1.136	91.46	0.90

0.88 to 0.96 indicated the validity of Yoon-Nelson model for the present system. As shown in the Table-7, k_{YN} values decreased from 1.94 to 1.13 min⁻¹ and the 50 % breakthrough time increased from 50.43 to 91.46 min as the bed depth increased from 10 to 20 cm. The value of ' τ ' significantly decreased ($p < 0.05$) from 120.3 to 25.64 min as the influent Cr(VI) concentration increased from 100 to 300 mg/L. In Yoon-Nelson model, the decrease in ' τ ' value was due to the rapid saturation of the column⁴³.

In a comparison of values of r^2 , both Thomas and Yoon-Nelson models can be used to predict adsorption performance for adsorption of Cr(VI) in a packed bed reactor.

Regeneration of column: Four subsequent cycles of alternating sorption/ desorption studies yielded 100, 99.51, 85.42 and 83.7 % regeneration of the sorbent. The sorption capacity at first and second cycle was not significantly different. As the cycles progressed from second to fourth, a significant decrease ($p < 0.05$; one-way analysis of variance and post test by Dunnett's Multiple Comparison Test) was noted. As the number of cycles proceeded it was found that the bed height also decreased. As the flow rate increases, the breakthrough time is less and the curve becomes steeper. This implies that the residence time for the metal ions inside the column has decreased resulting in less sorption due to insufficient sorption time. Hence, lower flow rates are ideal for increasing sorption capacity of the column. As the bed height increases, the surface area available for sorption of metal ions increases leading to an increase in the sorption capacity. The sorption capacities measured in the subsequent cycles indicated cumulative measure of the metal ions remaining adsorbed from the previous cycle after desorption and that resulted from the present

adsorption process. The decrease in bed height as the number of cycles proceeded may be due to the dissolution of some soluble constituents during the regeneration of biosorbent⁴⁴. The loss of biosorption performance is not mainly due to the biosorbent damage but rather because of sorption sites, whose accessibility became difficult as the cycles progressed. The regeneration percentage was more compared to earlier reports on biosorbent regeneration^{45,46}.

Application studies: From 300 mg/L Cr(VI) spiked ground water samples [collected from Soloor (GW1) and Suthipattu (GW2)], 55.64 and 51.67 % of Cr(VI) was removed by algal consortium immobilized alginate bead with adsorption capacity of 455.69 and 423.17 mg/g, respectively which was less than the adsorption capacity in deionized water matrix (579.2 mg/g). In 300 mg/L Cr(VI) spiked lake water and domestic waste water, 47.31 and 41.23 % Cr(VI) were removed, corresponding to 387.46 and 337.67 mg/g adsorption capacity, respectively. This suggests the application of algal consortium immobilized alginate bead for treating Cr(VI) in different water matrices.

In the tannery effluent samples collected from Soloor (T1) and Suthipattu (T2), the total chromium content was 638.8 and 545.15 mg/L, respectively. The Cr(III) is presumed to be prevalent species in the effluent samples and presence of Cr(VI) can be ignored¹⁶. To these samples, 300 mg/L Cr(VI) was spiked taking the total initial total Cr concentrations to 938.2 and 845 mg/L, respectively. From these samples, 28.01 and 27.57 % of total Cr was removed at adsorption capacity of 573.81 mg/g (T1) and 540.29 mg/g (T2). The adsorption capacity was less than that noted in distilled deionized water matrix (579.2 mg/g). The presence of Cr(III) in the tannery effluent had a mild effect on the sorption capacity of the sorbent. The high adsorption capacity of total Cr [Cr(VI) + Cr(III)] from the tannery effluents shows that the algal consortium immobilized alginate beads are efficient biosorbents for non site specific applications. Further studies are required to validate its application potential.

Conclusion

The present study shows that the immobilized algal consortium of *Oocystis sp*, *Nostoc sp*, *Syncoccus sp* and *Desimococcus sp* was capable of removing Cr(VI) from contaminated waters and effluents. The adsorption capacity increased to 83.53 mg/g in batch and 579.2 mg/g in column

reactor on immobilization of adapted freshwater algal consortium. Adsorption mediated surface reduction of Cr(VI) to Cr(III) was evident from the EDAX, FT-IR and EPR studies. The advantages of high biosorption capacity and reduction efficiency can be effectively exploited for scaling up of large scale reactors for continuous applications in contaminated sites.

ACKNOWLEDGEMENTS

The authors thank the Sophisticated Analytical Instrumentation Facility, (DST, India) at IIT, Madras for providing the instrumentation facility and also thank the management of VIT University for their support in research. JS and MLP acknowledge the Senior Research fellowship support from Council of Scientific & Industrial Research, India.

REFERENCES

1. S.V. Gokhale, K.K. Jyoti and S.S. Lele, *J. Hazard. Mater.*, **170**, 735 (2009).
2. S.K. Singh, A. Bansal, M.A. Jha and A. Dey, *Bioresour. Technol.*, **104**, 257 (2012).
3. A.H. Ullrich and M.W. Smith, *Ind. Wastes*, **23**, 1248 (1951).
4. J.M. Modak and K.A. Natarajan, *Miner. Metall. Proc.*, **121**, 89 (1995).
5. J.L. Zhou and R.J. Kiff, *J. Chem. Technol. Biotechnol.*, **52**, 317 (1991).
6. G. Yan and T. Viraraghavan, *Water S.A.*, **26**, 119 (2000).
7. O.R. Zimmo, R.A. Saed and H. Gijzen, *Water Sci. Technol.*, **42**, 215 (2000).
8. A. Ruiz-Marin, L.G. Mendoza-Espinosa and T. Stephenson, *Bioresour. Technol.*, **101**, 58 (2010).
9. P.S. Lau, N.F.Y. Tam and Y.S. Wong, *Environ. Technol.*, **18**, 945 (1997).
10. M.N. Kathiravan, R. Karthiga Rani, R. Karthick and K. Muthukumar, *Bioresour. Technol.*, **101**, 853 (2010).
11. B. Volesky and H.A. May Phillips, *J. Appl. Microbiol. Biotechnol.*, **42**, 797 (1995).
12. H.H. Tønnesen and J. Karlsen, *Drug Dev. Ind. Pharm.*, **28**, 621 (2002).
13. C. Bucke, *Methods Enzymol.*, **135**, 175 (1987).
14. P.K. Robinson and S.C. Wilkinson, *Enzyme Microb. Technol.*, **16**, 802 (1994).
15. P.S. Lau, N.F.Y. Tam and Y.S. Wong, *Bioresour. Technol.*, **63**, 115 (1998).
16. J. Samuel, M.L. Paul, M. Pulimi, M.J. Nirmala, N. Chandrasekaran and A. Mukherjee, *Ind. Eng. Chem. Res.*, **51**, 3740 (2012).
17. J. Samuel, M. Pulimi, M.L. Paul, A. Maurya, N. Chandrasekaran and A. Mukherjee, *Bioresour. Technol.*, **128**, 423 (2013).
18. N. Fiol, C. Escudero, J. Poch and I. Villaescusa, *React. Funct. Polym.*, **66**, 795 (2006).
19. K. Anjana, A. Kaushik, B. Kiran and R. Nisha, *J. Hazard. Mater.*, **148**, 383 (2007).
20. J. Bajpai, R. Shrivastava and A.K. Bajpai, *Colloids Surf. A*, **236**, 81 (2004).
21. A. Selatnia, M.Z. Bakhti, A. Madani, I. Kertous and Y. Mansouri, *Hydrometallurgy*, **75**, 11 (2004).
22. S.S. Baral, S.N. Das and P. Rath, *Biochem. Eng. J.*, **31**, 216 (2006).
23. M. Jain, V.K. Garg and K. Kadirvelu, *J. Environ. Manage.*, **91**, 949 (2010).
24. X. Hu, J. Wang, Y. Liu, X. Li, G. Zeng, Z. Bao, X. Zeng, A. Chen and F. Long, *J. Hazard. Mater.*, **185**, 306 (2011).
25. V.K. Gupta, A.K. Shrivastava and N. Jain, *Water Res.*, **35**, 4079 (2001).
26. M.L. Paul, J. Samuel, N. Chandrasekaran and A. Mukherjee, *Chem. Eng. J.*, **187**, 104 (2012).
27. B. Greene, M. Hosea, R. McPherson, M. Henzl, M.D. Alexander and D.W. Darnall, *Environ. Sci. Technol.*, **20**, 627 (1986).
28. Y.S. Chen, Q.J. Sun, J. Chen and Y.Y. Zhuang, *Adv. Environ. Sci.*, **5**, 34 (1997).
29. L.J. Bellamy, *The Infra-red Spectra of Complex Molecules*, Chapman and Hall, London, edn 3, p. 107 and 269 (1978).
30. R.M. Silverstein, G.C. Bassler and T.C. Morrill, in eds.: In: D. Sawicki and J. Stiefel, *Spectrometric Identification of Organic Compounds*, Wiley, New York, pp. 125 (1991).
31. W.J. Zhou and Y. Wang, in ed.: J.G. Wu, *Modern Fourier-Transform Infrared Spectroscopy and its Applications*, Literature of Science and Technology Press, Beijing, p. 273 (1994).
32. Z. Lin, Y. Ye, Q. Li, Z. Xu and M. Wang, *BMC Biotechnol.*, **11**, 98 (2011).
33. V. Daier, S. Signorella, M. Rizzotto, M.I. Frascaroli, C. Palopoli, C. Brondino, J.M. Salas-Peregrin and L.F. Sala, *Can. J. Chem.*, **77**, 57 (1999).
34. M. TamezUddin, M. Rukanuzzaman, M. MaksudurRahman Khan and M. Akhtarul Islam, *J. Environ. Manage.*, **90**, 3443 (2009).
35. N. Chen, Z.Y. Zhang, C.P. Feng, M. Li, R.Z. Chen and N. Sugiura, *Desalination*, **268**, 76 (2011).
36. S.S. Baral, N. Das, T.S. Ramulu, S.K. Sahoo, S.N. Das and G.R. Chaudhury, *J. Hazard. Mater.*, **161**, 1427 (2009).
37. E. Malkoc, Y. Nuhoglu and Y. Abali, *Chem. Eng. J.*, **119**, 61 (2006).
38. R. Vimala, D. Charumathi and N. Das, *Desalination*, **275**, 291 (2011).
39. B. Preetha and T. Viruthagiri, *Sep. Purif. Technol.*, **57**, 126 (2007).
40. R. Han, Y. Wang, X. Zhao, Y. Wang, F. Xie, J. Cheng and M. Tang, *Desalination*, **245**, 284 (2009).
41. A.A. Ahmad and B.H. Hameed, *J. Hazard. Mater.*, **175**, 298 (2010).
42. Z. Aksu, F. Gönen and Z. Demircan, *Process Biochem.*, **38**, 175 (2002).
43. M. Calero, F. Hernández, G. Blázquez, G. Tenorio and M.A. Martín-Lara, *J. Hazard. Mater.*, **171**, 886 (2009).
44. R. Senthilkumar, K. Vijayaraghavan, M. Thilakavathi, P.V.R. Iyer and M. Velan, *J. Hazard. Mater.*, **136**, 791 (2006).
45. P. Suksabye, P. Thiravetyan and W. Nakbanpote, *J. Hazard. Mater.*, **160**, 56 (2008).
46. R. Kumar, D. Bhatia, R. Singh, S. Rani and N.R. Bishnoi, *Int. Biodeter. Biodegr.*, **65**, 1133 (2011).
47. V.K. Gupta, A.K. Shrivastava and N. Jain, *Water Res.*, **35**, 4079 (2001).
48. H. Li, T. Liu, Z. Li and L. Deng, *Bioresour. Technol.*, **99**, 2234 (2008).
49. L. Deng, Y. Zhang, J. Qin, X. Wang and X. Zhu, *Miner. Eng.*, **22**, 372 (2009).
50. A. El-Sikaily, A.E. Nemr, A. Khaled and O. Abdelwehab, *J. Hazard. Mater.*, **148**, 216 (2007).
51. S. Chen, Q. Yue, B. Gao, Q. Li, X. Xu and K. Fu, *Bioresour. Technol.*, **113**, 114 (2012).
52. M.G.A. Vieira, R.M. wOisiovici, M.L. Gimenes and M.G.C. Silva, *Bioresour. Technol.*, **99**, 3094 (2008).
53. L. Deng, Y. Su, H. Su, X. Wang and X. Zhu, *J. Hazard. Mater.*, **143**, 220 (2007).
54. S.V. Gokhale, K.K. Jyoti and S.S. Lele, *Bioresour. Technol.*, **99**, 3600 (2008).